Available online at www.sciencedirect.com
SCIENCE DIRECT
Cement and Concrete Research 35 (2005) 2300–2309
Cement and Concrete Research

Hydrothermal transformation of the calcium aluminum oxide hydrates $CaAl_2O_4 \cdot 10H_2O$ and $Ca_2Al_2O_5 \cdot 8H_2O$ to $Ca_3Al_2(OH)_{12}$ investigated by in situ synchrotron X-ray powder diffraction

Torben R. Jensen[a,*], Axel Nørlund Christensen[b], Jonathan C. Hanson[c]

[a]*Interdisciplinary Nanoscience Center, Department of Chemistry, University of Aarhus, Langelandsgade 140, DK-8000 Aarhus C, Denmark*
[b]*Højkolvej 7, DK-8210 Århus V, Denmark*
[c]*Chemistry Department, Brookhaven National Laboratory, Upton, NY 11973, USA*

Received 16 June 2004; accepted 28 October 2004

Abstract

The hydrothermal transformation of calcium aluminate hydrates were investigated by in situ synchrotron X-ray powder diffraction in the temperature range 25 to 170 °C. This technique allowed the study of the detailed reaction mechanism and identification of intermediate phases. The material $CaAl_2O_4 \cdot 10H_2O$ converted to $Ca_3Al_2(OH)_{12}$ and amorphous aluminum hydroxide. $Ca_2Al_2O_5 \cdot 8H_2O$ transformed via the intermediate phase $Ca_4Al_2O_7 \cdot 13H_2O$ to $Ca_3Al_2(OH)_{12}$ and gibbsite, $Al(OH)_3$. The phase $Ca_4Al_2O_7 \cdot 19H_2O$ reacted via the same intermediate phase to $Ca_3Al_2(OH)_{12}$ and mainly amorphous aluminum hydroxide. The powder pattern of the intermediate phase is reported.

Keywords: Hydration products; Calcium aluminate cement; Hydrogarnet; X-ray diffraction

1. Introduction

The calcium aluminates $Ca_3Al_2O_6$ (C_3A), $Ca_{12}Al_{14}O_{33}$ ($C_{12}A_7$), and $CaAl_2O_4$ (CA), are the most reactive aluminates in the hydration of Portland cements and calcium aluminate cements [1,2]. In the hydraulic reactions, a number of metastable hydrated phases as $CaAl_2O_4 \cdot 10H_2O$ (CAH_{10}), $Ca_2Al_2O_5 \cdot 8H_2O$ (C_2AH_8), and $Ca_4Al_2O_7 \cdot xH_2O$ (x=7, 11, 13 and 19) can be formed depending upon the reaction temperatures and solution composition [1–5]. Many of these phases can be observed in the microscope as hexagonal crystals [3], but their crystal structures are not known in great detail. The only stable hydrated calcium aluminate is the cubic calcium aluminum hydroxide $Ca_3Al_2(OH)_{12}$ (C_3AH_6) with a garnet structure [6]. This compound is an end product in the hydration of the calcium aluminates [7–13].

The hydrated calcium aluminate phases may be identified from their X-ray powder diffraction patterns [4]. The powder pattern of C_3AH_6 was reported as early as in 1929 [14]. The phase C_2AH_8 was obtained much earlier, in 1900, in reaction at room temperature of aluminum metal with a saturated aqueous solution of calcium hydroxide, and from chemical analysis the composition $Ca_2Al_2O_5 \cdot 7H_2O$ was deduced [15]. The powder patterns of CAH_{10} and C_2AH_8 were reported in 1933 as stick diagrams in the d-spacing range 1–7 Å [16] and the compound C_4AH_x (x=13.5) was made at 40 °C in 1932 [17]. Several different hydrates and polymorphs of C_4AH_x (x=7, 11, 13 and 19) and C_2AH_x (x=4, 5, 7.5 and 8) were reported in 1957 [18]. Only the two compounds C_4AH_{19} and C_2AH_8 were present in aqueous media: the remaining phases were produced on drying under various conditions. The different hydrated states manifested

* Corresponding author. Tel.: +45 8942 3894; fax: +45 8619 6199.
E-mail address: trj@chem.au.dk (T.R. Jensen).

0008-8846/$ - see front matter © 2004 Elsevier Ltd. All rights reserved.
doi:10.1016/j.cemconres.2004.10.034

themselves by changes in the *c*-axis or the interlayer spacing, while the *a*- and *b*-axes were slightly affected. Only the longest *d*-spacings of the powder patterns were reported, for C_4AH_x (x=7, 11, 13 and 19) the values 7.4, 7.4, 8.2, 7.9 and 10.6 Å, respectively, and for C_2AH_x (x=4, 5, 7.5, and 8) the values 7.4, 8.7, 10.6, 10.7 and 10.4 Å, respectively. However, for the phases C_2AH_8 and C_4AH_{19}, the *d*-spacings at 10.7 and 5.36 Å match for both compounds [11], which makes it difficult to determine unambiguously if the two compounds are present as pure phases or as mixtures. The two hydrates are formed in hydration of C_3A according to the reaction [11],

$$2C_3A + 27H \rightarrow C_2AH_8 + C_4AH_{19} \quad (1)$$

The identification of the different hydrated calcium aluminate phases is difficult due to the lack of reliable crystallographic data and the structural similarities in these phases, giving similar powder diffraction patterns. The phase C_2AH_8 is identified by the JCPDS card # 45-564, which also reports excellent agreement between the chemical formula, $CaAl_2O_5 \cdot 8H_2O$, and the analytical composition (CaO: 31.3%, Al_2O_3: 25.5%, and H_2O: 40.2%). The phase C_4AH_{19} is identified by # 42-487, where acceptable agreement with the chemical formula, $Ca_4Al_2O_7 \cdot 19H_2O$, is found for the analytical composition (CaO: 33.7%, Al_2O_3: 14.9%, and H_2O: 51.2%). In contrast, for the phases C_2AH_x and C_4AH_x with x less than 8 and 19, respectively, only the *d*-spacings at low Bragg angles are reported [4,18].

C_2AH_8 can be made as a pure phase in hydration of a mixture of C_3A and $C_{12}A_7$, present in a calcium aluminate mix with the nominal composition $Ca_2Al_2O_5$ [19], according to the reaction

$$C_2A + 8H \rightarrow C_2AH_8 \quad (2)$$

The hydrated calcium aluminate CAH_{10} is obtained at temperatures below 15 °C in hydration of CA as described in reaction scheme (3) below [2]

$$CA + 10H \rightarrow CAH_{10} \quad (3)$$

The hydration of Portland cement and of the calcium aluminates C_3A and $C_{12}A_7$ have recently been investigated by in situ synchrotron X-ray powder diffraction [20]. The investigations were made at hydrothermal conditions at temperatures up to 170 °C. In continuation of this work, it was decided to study the hydrothermal formation of C_3AH_6 from the metastable hydrated phases CAH_{10} and C_2AH_8/C_4AH_{19}. The slow transformations of the metastable phases to the stable product are accelerated by the temperature and pressure increase at hydrothermal conditions. The in situ studies obviate the necessity of extrapolation from experimental to ambient conditions and remove artefacts possibly induced in ex situ investigations such as phase or composition changes. The results of the present investigation are reported below.

2. Experimental

The solid state synthesis of calcium aluminates from the pure chemicals $CaCO_3$ (Merck p.a.) and $Al(OH)_3 \cdot 0.949H_2O$ (Aldrich) is described previously [20,21]. The compounds CA, C_3A, and a C_3A–$C_{12}A_7$ mixture with the nominal composition C_2A were ground in a boron carbide mortar, passed through a 0.112 mm sieve and stored in air tight plastic flask at ~20 °C. The C_2A sample had the molar composition: $C_{12}A_7$ 78%, C_3A 22%. The in situ hydration reactions occurred in 0.7 mm capillaries; distilled water containing less than 0.01% of a detergent was used. The detergent reduces the surface tension of water and ensures an efficient and fast wetting of the solid powders.

2.1. Sample A, CAH_{10} made from CA

The sample was made from hydration of CA at experimental conditions resulting in the compound CAH_{10} [19], see reaction (2). CA (7.5 g) was mixed with 50 mL of the above-mentioned solution in a 100 mL glass flask at 2 °C, stirred with a magnetic stirrer and kept at 2 °C for 18 days. The CA/water mixture was a suspension throughout the reaction period. The product was filtered on a glass filter, washed with water and dried at ~20 °C over silica gel. An X-ray powder pattern recorded of the wet paste on a Stoe Stadi diffractometer using Cu $K\alpha_1$ radiation (λ=1.540598 Å) [20,21] showed that the reaction product was CAH_{10} (JCPDS card # 12-408). The product was dried at ambient conditions and another X-ray powder patterns confirmed that the structure was preserved as CAH_{10}.

2.2. Sample B, C_2AH_8/C_4AH_{19} made from C_3A

The sample was made by hydration of C_3A at conditions described below, resulting in the compounds C_2AH_8 and C_4AH_{19} [11], see reaction (1). A C_3A-H_2O paste was made from 0.5 g C_3A and 2 mL water in a small glass flask, and the paste was kept in the closed flask at 2 °C for 330 h. The paste was stirred occasionally until it became solid. The sample was crushed in a mortar, washed with water and filtered and dried in air at room temperature and kept in a plastic flask. An X-ray powder pattern of the sample shows that it contained several phases: the position of the Bragg reflections corresponded to the *d*-spacings of $Ca_2Al_2O_5 \cdot 8H_2O$, $Ca_4Al_2O_7 \cdot 19H_2O$, $Ca_2Al_2O_5 \cdot 10H_2O$, and $Ca_4Al_2O_7 \cdot xH_2O$ (JCPDS cards # 45-564, 42-487, 16-339 and 2-77, respectively). In addition, the sample contained an impurity of C_3A (JCPDS card # 38-1429). The match with card # 2-77 was not perfect, and this card does possibly not represent the powder pattern of a pure phase of calcium aluminate hydrate.

2.3. Sample C, C_2AH_8 made from C_2A

The sample was made by hydration of C_2A at conditions resulting in the compound C_2AH_8 [19], see reaction (3); 7.5 g of the C_2A sample was mixed with 50 mL of the above-mentioned liquid in a 100 mL plastic flask at 25 °C, stirred occasionally and kept at 25 °C for 36 h. The C_2A/water mixture was a suspension throughout the reaction period. The sample was treated as described above for CAH_{10}. An X-ray powder pattern recorded of the wet paste of the sample was in agreement with JCPDS card # 42-487 for C_4AH_{19}, and an X-ray powder pattern recorded of the sample dried for 60 days at room temperature showed Bragg reflections for C_4AH_{19} and C_4AH_{13}, JCPDS cards # 42-487 and 33-255.

2.4. In situ investigation

The time-resolved synchrotron X-ray diffraction data were collected on beam line X7B of the National Synchrotron Light Source (NSLS) using a MAR345 area detector. The samples were placed in 0.7 mm diameter quartz glass capillaries and heated in a hot air stream. The reactions studied are in some cases relatively fast, e.g. within the first minutes after addition of water, necessitating development of a new technique for in situ experiments. The solid sample was placed at the tip of the capillary with a height of 1–2 mm. Water was placed in the capillary with a syringe using a 0.5 mm quartz glass capillary as needle, so that ca. 1 mm air separate the water and the solid, and the water/solid ratio was ca. 10:1. A few powder patterns were collected before the capillary was pressurized ($p(N_2) \approx 1700$ kPa), which caused an immediate wetting of the solid sample when in contact with the water and ensured that water vapour bubbles did not form in the hydrothermal liquid. The nitrogen pressure reduces the air volume in the sample by approximately 90%, then the solid phase and liquid phase in the sample are mixed and the water/solid ratio (ca. 10:1) ensures sufficient water for the reaction. The water contained less than 0.01% of a detergent, which reduced the surface tension considerably. Temperature ramps from 25 to 120 °C and from 25 to 170 °C were used with heating rates of 0.79 and 1.21 °C/min, respectively. Each pattern is recorded in a small temperature interval determined by the temperature ramp and the X-ray exposure time of the pattern. The selected X-ray wavelengths were λ=0.92018 and 0.92274 Å refined with a

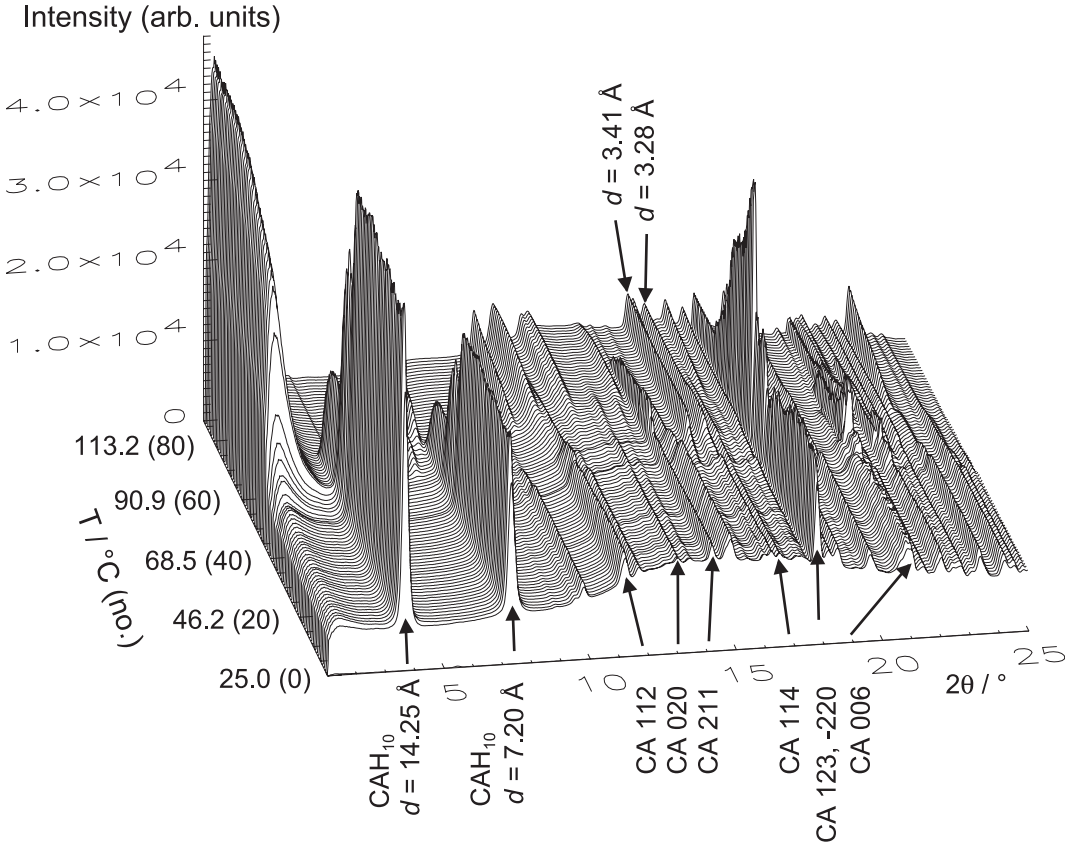

Fig. 1. Stack of powder patterns of CAH_{10} containing CA, sample A, hydrated in a temperature ramp from 25 to 120 °C and recorded using synchrotron radiation, λ=0.92018 Å. Positions of CA reflections are marked with Miller indices, and positions of two strong CAH_{10} reflections are marked with their d-spacings.

powder pattern of LaB_6 (a=4.1570 Å). The capillaries were oscillated 10° to randomize the orientations of the crystallites in the samples. The diffraction data frames from the MAR345 area detector were converted to powder patterns with the software FIT2D [22], giving a 2θ range of 0 to 38°, with $\sin(\theta/\lambda)_{max}$=0.354.

3. Results

3.1. CAH_{10} hydrothermal treatment of sample A

The hydrothermal treatment of the CAH_{10}–water mixture was recorded with slow heating rate, 1.10 °C per powder pattern; Fig. 1 shows a stack of powder patterns in the 2θ range 1° to 25°. The solid sample was $CaAl_2O_4 \cdot 10H_2O$ with an impurity of unreacted CA. The positions of the two strong $CaAl_2O_4 \cdot 10H_2O$ reflections at d=14.25 and 7.20 Å and seven CA reflections are indicated.

In pattern nos. 1–37 (25–65 °C), no significant changes in the intensities of the Bragg reflections are observed. In pattern nos. 38–46 (66–75 °C), an increase in the background levels is observed in the 2θ range 1° to 3°. The background increases with depletion of CAH_{10}. A general change in the background level is observed as a relative increase of the intensity of the strong 211, 123, $\bar{2}20$, and 006 CA reflections, and in addition Bragg reflections of another phase are observed with the d-spacings 3.41 and 3.28 Å. Additional intermediate phases are formed; one is observed in pattern nos. 48–63 (77–93 °C) and another in pattern nos. 58–87 (88–120 °C). The final reaction product, C_3AH_6, is observed in pattern nos. 58–87 (88–120 °C). This is clearer in Fig. 2 displaying pattern nos. 43–84 (72–117 °C) in the 2θ range 1° to 19°. The Bragg reflections of CAH_{10} are not present after pattern no. 59 (89 °C), and the Bragg reflections of CA are not present after pattern no. 73 (105 °C). The phase having Bragg reflections at d=3.41 and 3.28 Å is present up to 120 °C, but this phase has not been identified.

The intermediate phase with Bragg reflections at d=8.13 Å is interpreted as C_2AH_{10}, (JCPDS card # 16-339), and the intermediate phase with Bragg reflections at the d-spacings 7.66, 4.83, 4.37 and 3.82 Å is interpreted as C_4AH_{13} (JCPDS card # 33-255). The positions of the Bragg reflections of the final stable product, C_3AH_6, are

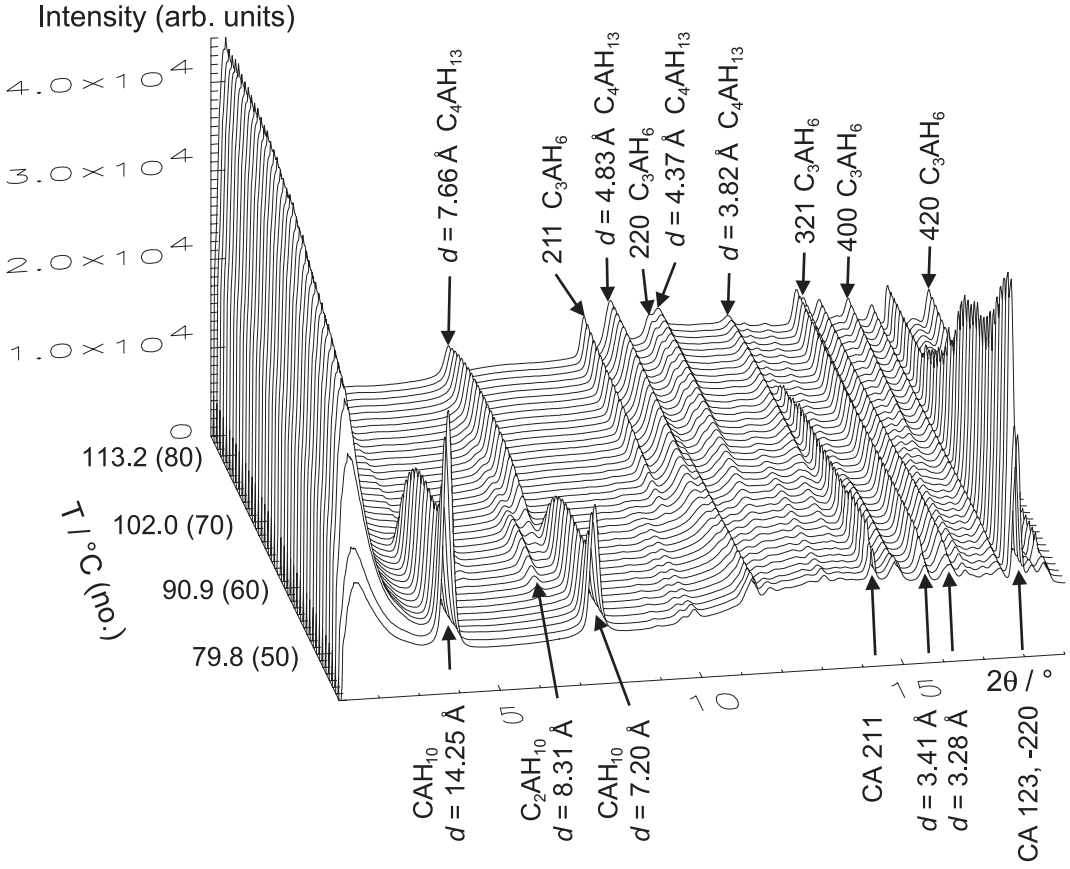

Fig. 2. Stack of powder patterns of CAH_{10} containing CA, sample A, hydrated in the temperature ramp 72 to 117 °C, a section of the stack displayed in Fig. 1. Positions of CA and CAH_{10} reflections are marked. The reflection at d=8.13 Å most likely belongs to a C_2AH_{10} phase (JCPDS card # 16-339). Two reaction products are observed at 117 °C. A phase with reflections at d=7.66, 4.83, 4.37, and 3.82 Å, which possibly belongs to C_4AH_{13} (JCPDS card # 33-255), and the end product C_3AH_6 where the reflections are marked with Miller indices.

indicated by their Miller indices. The chemical reactions in the transformation of CA and CAH_{10} to C_3AH_6 are:

$$CaAl_2O_4 + 10H_2O \rightarrow CaAl_2O_4 \cdot 10H_2O \quad (4)$$

$$4CaAl_2O_4 \cdot 10H_2O \rightarrow Ca_4Al_2O_7 \cdot 13H_2O + 6Al(OH)_3(\text{amorphous}) + 18H_2O \quad (5)$$

$$2CaAl_2O_4 \cdot 10H_2O \rightarrow Ca_2Al_2O_5 \cdot 10H_2O + 2Al(OH)_3(\text{amorphous}) + 7H_2O \quad (6)$$

$$2Ca_2Al_2O_5 \cdot 10H_2O \rightarrow Ca_4Al_2O_7 \cdot 13H_2O + 2Al(OH)_3(\text{amorphous}) + 4H_2O \quad (7)$$

$$Ca_4Al_2O_7 \cdot 13H_2O \rightarrow Ca_3Al_2(OH)_{12} + Ca(OH)_2 + 6H_2O \quad (8)$$

$$3Ca(OH)_2 + 2Al(OH)_3 \rightarrow Ca_3Al_2(OH)_{12} \quad (9)$$

3.2. C_2AH_8/C_4AH_{19} hydrothermal treatment of sample B

The hydrothermal treatment of the C_2AH_8/C_4AH_{19}–water mixture was recorded in the 2θ range 0–38° using a wavelength λ=0.92018 Å. A temperature ramp from 25 to 170 °C was used, and a total of 49 patterns were recorded corresponding to an increment in temperature of 3.0 °C per powder pattern.

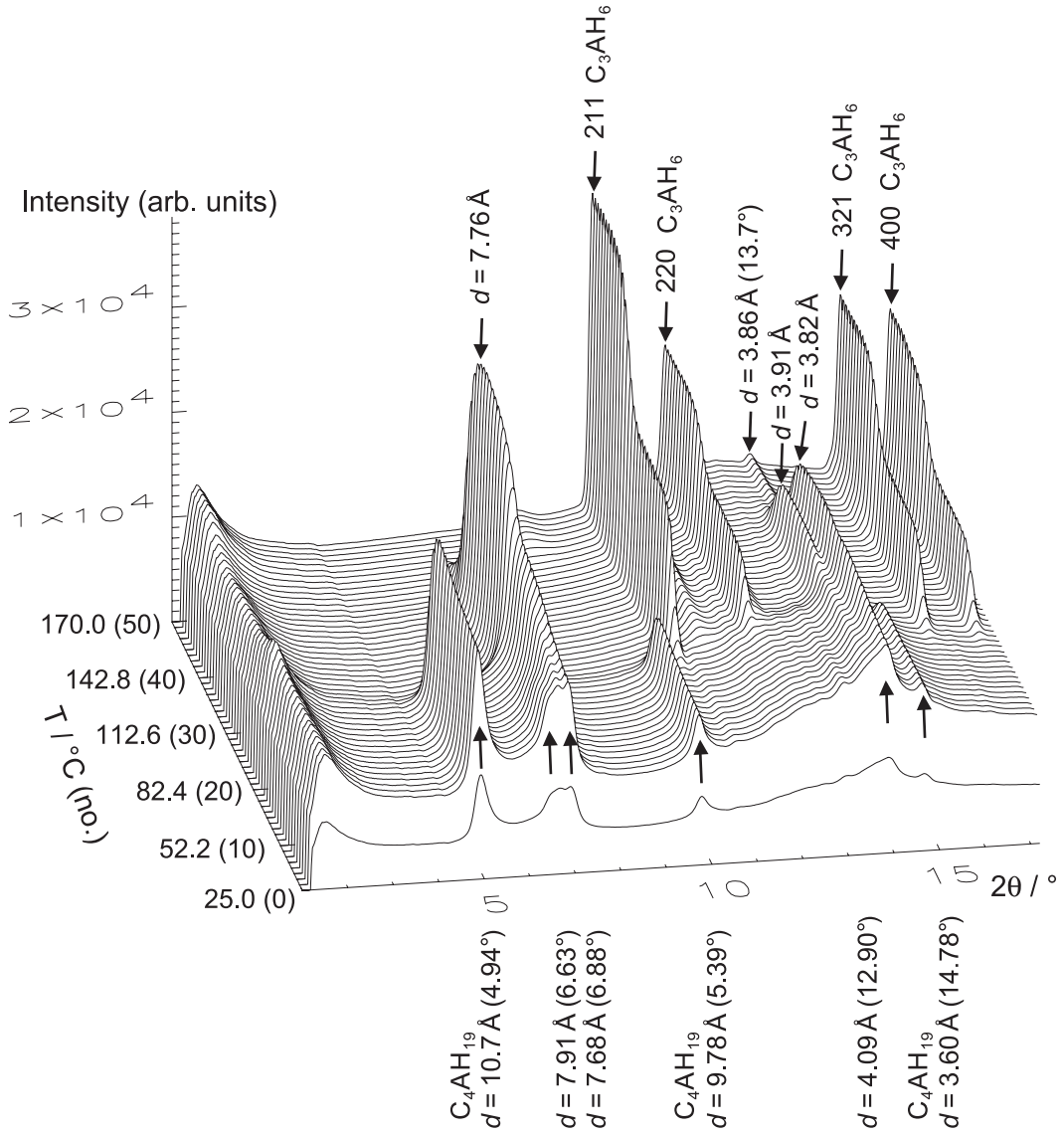

Fig. 3. Stack of powder patterns of a C_2AH_x/C_4AH_x mixture, sample B, in the 2θ range 1° to 17.2°, treated at hydrothermal conditions in a temperature ramp from 25 to 170 °C, and recorded using synchrotron radiation, λ=0.92018 Å. Positions of C_4AH_{19} and C_2AH_{10} reflections are marked for the first pattern recorded. Positions of reflections of the intermediate phase C_4AH_{13} are marked with the *d*-spacing values 7.76, 3.91, and 3.82 Å, and positions of reflections of the end product C_3AH_6 are marked with Miller indices.

Fig. 3 shows a stack of powder patterns of the mixture in the 2θ range 1° to 17.2°, and Fig. 4 in the 2θ range 17.2° to 35°. If the solid had been formed in the hydration reaction from C_3A reported in Ref. [11], it would consist of a mixture of C_2AH_8 and C_4AH_{19}. However, the hydration reaction of C_3A could also result in the formation of C_4AH_x (x=11, 13 or 19) and amorphous aluminum hydroxide, and this is most likely the case in the present investigation. It is obvious that the sample contains at least three solid phases. The patterns in Fig. 3 have an amorphous background in the 2θ range 2° to 3° and possibly also at in the 2θ range 13° to 16°. The Bragg reflections at the 2θ values 4.94°, 9.78° and 14.78° have the intensities 100, 30 and 10, which corresponds more closely to the intensities of the three reflections of C_4AH_{19} (JCPDS card # 42-487) of 100, 20 and 12, than the intensities of the three reflections of C_2AH_8 (JCPDS card # 45-564) of 100, 72 and 38. These three reflections of C_4AH_{19} are observed in pattern nos. 1–19 and are then depleted in the formation of the end product C_3AH_6, whose Bragg reflections can be observed from pattern no. 16 (at 70 °C). Simultaneously, the background intensity increases at low Bragg angles, 2θ=1–3°, suggesting an increasing amount of amorphous material. The positions of the Bragg reflections of C_3AH_6 are marked with their Miller indices. The chemical reactions in the transformation of C_4AH_{19} and C_2AH_8 to C_3AH_6 are described by reactions (10) and (11) below and subsequently by reaction schemes (8) and (9).

$$3Ca_4Al_2O_7\cdot 19H_2O + 2Al(OH)_3(\text{amorphous}) \rightarrow 4Ca_3Al_2(OH)_{12} + 36H_2O \quad (10)$$

$$2Ca_2Al_2O_5\cdot 8H_2O \rightarrow Ca_4Al_2O_7\cdot 13H_2O + 2Al(OH)_3(\text{amorphous}) \quad (11)$$

The first powder patterns of Figs. 3 and 4 have additional Bragg reflections at the 2θ positions 6.63°,

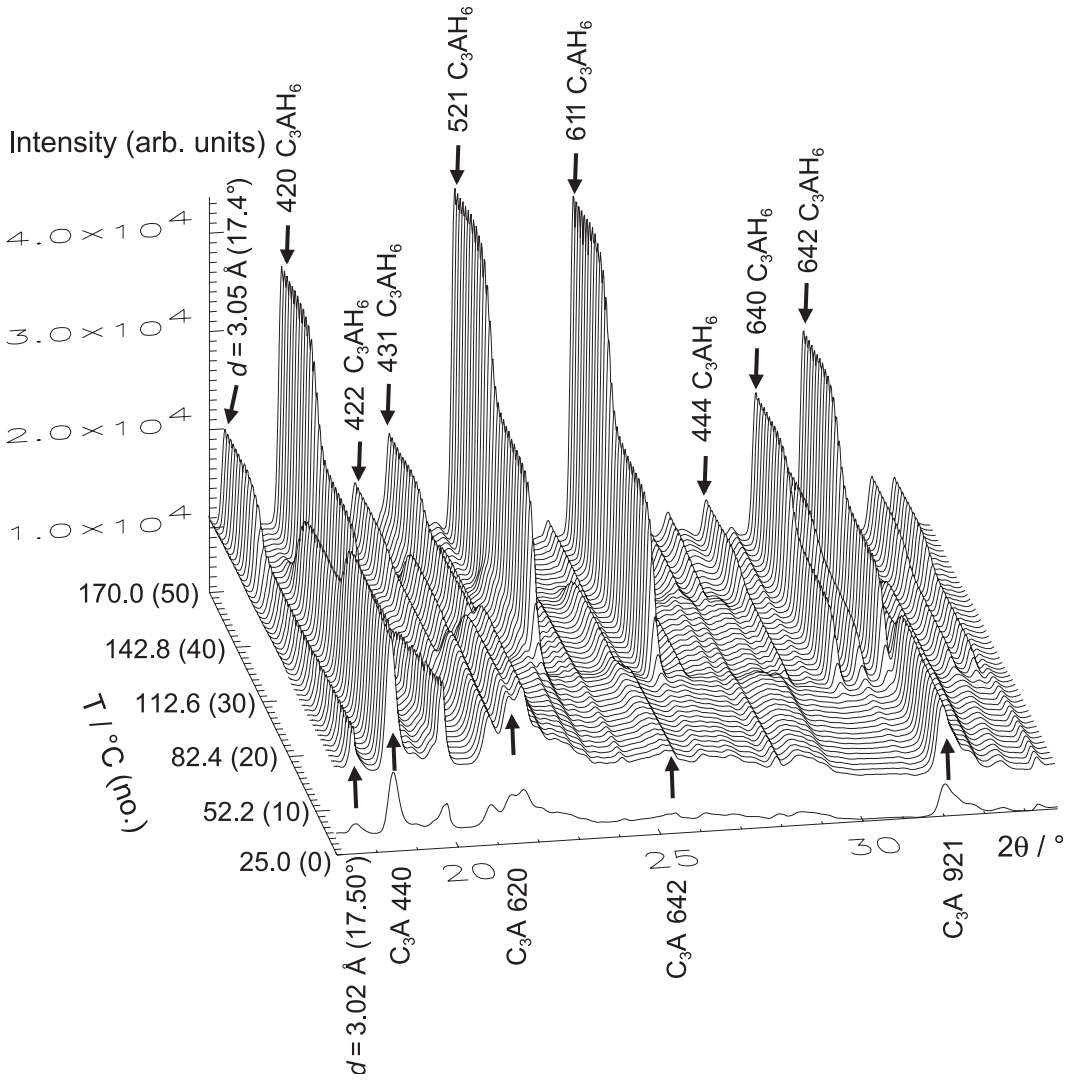

Fig. 4. Stack of powder patterns of a C_2AH_x/C_4AH_x mixture, sample B, in the 2θ range 17.2° to 35°, same experiment as displayed in Fig. 3. Positions of C_3A reflections are marked with Miller indices for the first pattern recorded, and positions of the end product C_3AH_6 are marked with Miller indices.

6.88°, 12.9°, and 17.50°, corresponding to the *d*-spacings 7.96, 7.68, 4.09, and 3.02 Å. These Bragg reflections possibly belong to C_2AH_x and C_4AH_x phases as observed previously [8]. In addition, Bragg reflections of C_3A are marked in Fig. 4. The reflections are depleted in two steps, one step in pattern nos. 16–21 (70–85 °C), and one in the pattern nos. 34–40 (125–143 °C); this is coupled with an increase in the C_3AH_6 Bragg intensities at pattern nos. 16–21 (70–85 °C) and in pattern nos. 32–36 (119–131 °C). Some of the C_2AH_x and C_4AH_x reflections are present in pattern nos. 18–37 (76–134 °C) with maxima at pattern no. 32 (119 °C) with the *d*-values 7.61, 3.91, and 3.82 Å. Simultaneously, with the increasing intensities of the C_3AH_6 Bragg reflections in pattern nos. 32–36, the amorphous background at 2θ=1 to 3° starts to increase and an additional crystalline phase is observed in the powder pattern no. 44 (155 °C) with Bragg reflections at the 2θ positions, 13.7°, and 17.4° corresponding to the *d*-spacings 3.86, and 3.05 Å. This phase has not been identified.

3.3. C_2A hydrothermal hydration

The hydration reaction of C_2A is reported to yield the compound C_2AH_8 [19], according to reaction (2), and thus corresponding to the formation reaction of sample C and its final composition. The solid C_2A sample had the molar composition: $C_{12}A_7$, 78% and C_3A, 22%. The in situ hydration of the C_2A sample was recorded in the 2θ range 0° to 50° using a wavelength of λ=0.92274 Å. A temperature ramp from 25 to 120 °C was used with an increment in temperature of 2.11 °C per pattern for pattern nos. 38–84. Pattern nos. 1–38 were recorded at 25 °C, and pattern nos. 84–108 were recorded at 120 °C. Fig. 5 displays a stack of powder patterns of the mixture in the 2θ range 1° to 17.2°. Pattern nos. 1 and 2 are recorded for the dry solid sample, and positions of 10 $C_{12}A_7$ and C_3A reflections are indicated. During the recording of pattern no. 3, water was introduced to the solid sample by applying nitrogen gas pressure to the sample in the quartz capillary, as described previously [20,21]. Pattern nos. 4–34 show formation of the first

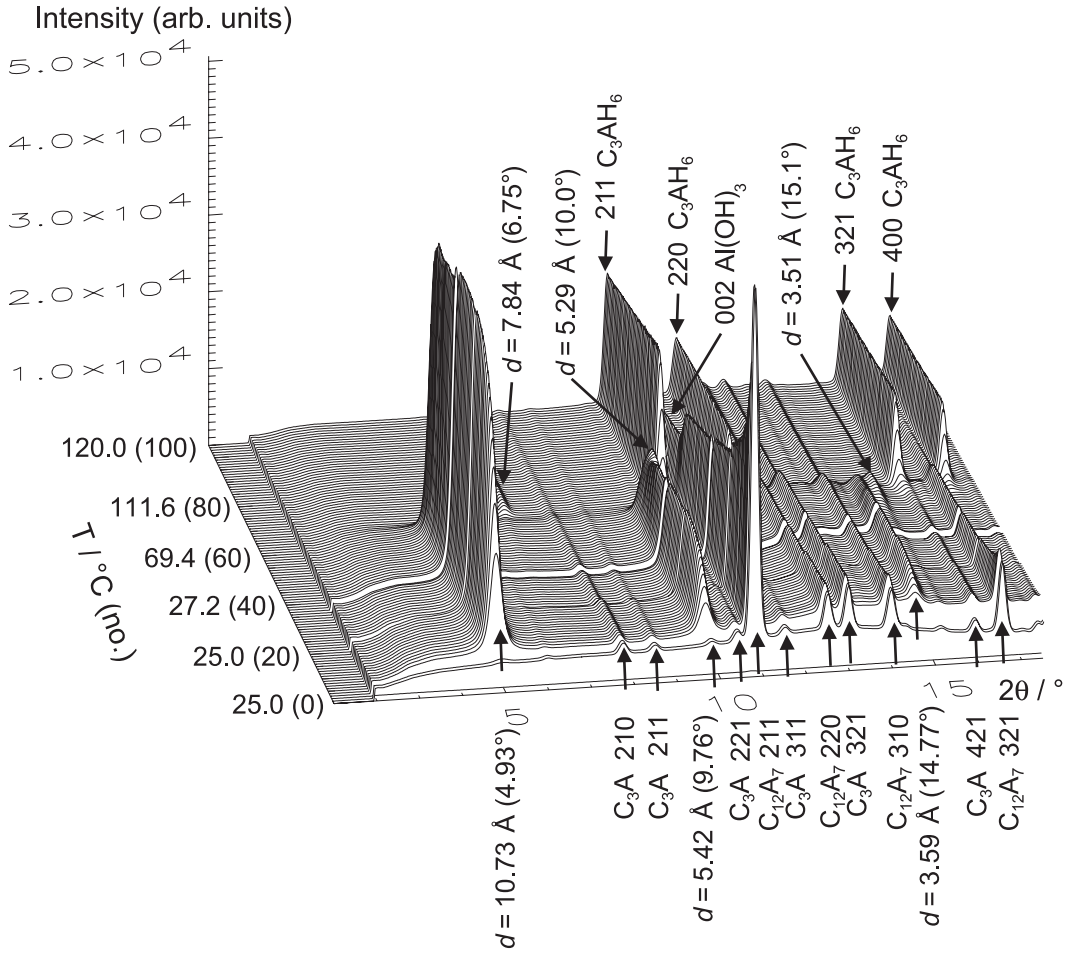

Fig. 5. Stack of powder patterns of a sample of C_2A, a mixture of C_3A and $C_{12}A_7$, in a hydrothermal hydration in the temperature ramp 25 to 120 °C, from nos. 38–84, recorded using synchrotron radiation, λ=0.92274 Å. Positions of C_3A and $C_{12}A_7$ reflections are indicated with Miller indices, and positions of three C_2AH_8 reflections are indicated with the *d*-spacings 10.73, 5.43, and 3.59 Å. Positions of an intermediate phase are marked by the *d*-spacings 5.29 and 3.51 Å, and of a minor quantity of C_4AH_{13} by the *d*-spacing 4.84 Å. The end product C_3AH_6 is marked by Miller indices.

reaction product in depletion of $C_{12}A_7$, indicated by the positions of the Bragg reflections of C_2AH_8 at the 2θ positions 4.93°, 9.76°, and 14.77°, corresponding to *d*-spacings 10.73, 5.42 and 3.59 Å. C_2AH_8 is assumed to be the reaction product according to reaction (2). However, the relative intensities of the three reflections are 100, 28, and 9, which is not in agreement with the JCPDS card # 45-564 for C_2AH_8. Heating of the sample was started between pattern nos. 37 and 38, C_2AH_8 occurs up to pattern no. 62 at 74 °C. A second intermediate phase is observed in pattern nos. 43 to 56 (34 to 61 °C) with *d*-spacings 5.29 and 3.51 Å, and is interpreted as C_4AH_{19}. A third reaction product is seen in pattern nos. 58–108 (65 to 120 °C) with the *d*-spacings at 7.84 Å, corresponding to C_4AH_{13}. The final stable reaction product C_3AH_6 has Bragg reflections in pattern nos. 55 to 108 (65 to 120 °C) and is indicated by Miller indices for C_3AH_6. In addition, the broad 002 reflection of gibbsite was observed at 2θ=10.9°. The chemical reactions in the hydrothermal transformation of the $C_{12}A_7$–C_3A mixture to C_3AH_6, where the mixture corresponds to the composition $Ca_2Al_2O_5$, are:

$$Ca_2Al_2O_5 + H_2O \rightarrow Ca_2Al_2O_5 \cdot 8H_2O \quad (12)$$

$$3Ca_2Al_2O_5 \cdot 8H_2O \rightarrow 2Ca_3Al_2(OH)_{12} + 2Al(OH)_3 + 9H_2O \quad (13)$$

3.4. C_2AH_8 hydrothermal treatment of sample C

The hydrothermal treatment of the C_2AH_8–water mixture was recorded in the 2θ range 0° to 38° using

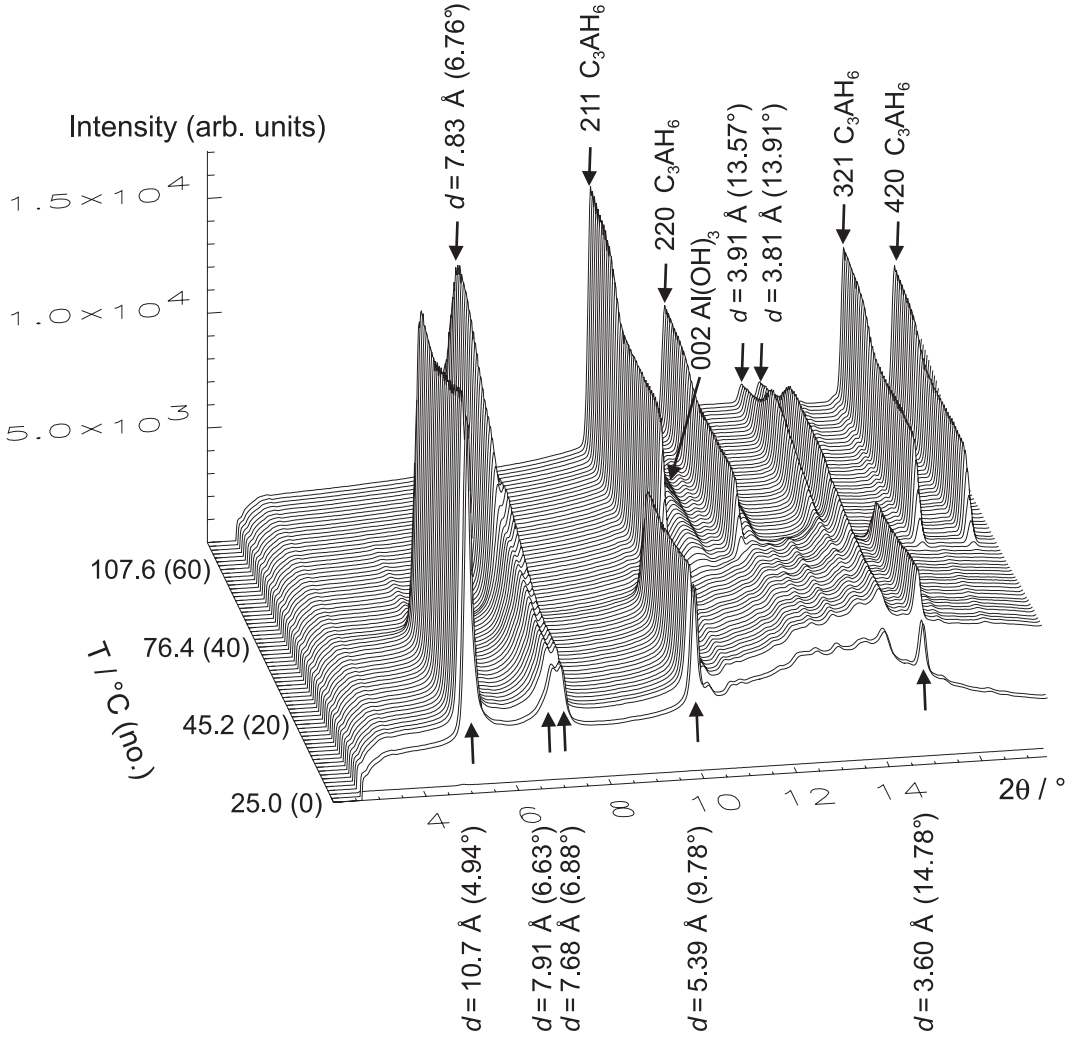

Fig. 6. Stack of powder patterns of the C_2AH_8–water mixture, sample C, in the 2θ range 2° to 17.2°, heated in the temperature ramp 25 to 120 °C, and recorded using synchrotron radiation, λ=0.92274 Å. Pattern nos. 1 to 2 are recorded with the dry solid sample showing Bragg reflections of C_2AH_8, C_2AH_{10} and C_4AH_{13}. During recording of pattern no. 3, water was introduced to the sample which can be observed as an increase in the background of the following patterns. C_2AH_8 is present in the patterns up to no. 30 (61 °C) and the intensity of the C_2AH_{10} and C_4AH_{13} reflections at *d*=7.91 and 7.68 Å, respectively, increase gradually up to pattern no. 32 (64 °C) where the intensity of the C_4AH_{13} reflections has its maximum. The end product C_3AH_6 is marked by Miller indices.

Table 1
Powder pattern of C_4AH_{13}, pattern no. 40, recorded at 76 °C, and λ=0.92274 Å

d (Å)	2θ (°)	I_{obs}
7.83	6.76	100
4.84	10.93	9
4.76	11.13	8
3.905	13.57	23
3.810	13.91	25
3.045	17.43	4
2.883	18.42	30
2.523	21.07	23
2.443	21.77	22
2.204	24.17	6
2.120	25.14	15
1.956	27.29	3
1.931	27.65	6
1.900	28.11	3
1.862	28.70	3
1.818	29.41	5
1.780	30.05	1
1.664	32.19	14
1.627	32.94	9
1.530	35.10	4
1.468	36.63	6
1.441	37.34	5
1.385	38.94	1
1.261	42.92	1
1.192	45.53	1

a wavelength of λ=0.92274 Å. A temperature ramp from 25 to 120 °C was used and a total of 68 patterns were recorded with an increment in temperature of 1.56 °C per pattern.

Fig. 6 displays a stack of powder patterns of the mixture in the 2θ range 0° to 17°. Pattern nos. 1 to 2 are recorded with the dry solid sample showing Bragg reflections of C_2AH_8, C_2AH_{10} and C_4AH_{13}. This is very similar to the observations depicted in Fig. 3. During recording of pattern no. 3, water was introduced, which can be observed as an increase in the background of the subsequent patterns. C_2AH_8 is present in the patterns up to no. 30 (61 °C) and the intensity of the C_2AH_{10} and C_4AH_{13} reflections at d=7.91 and 7.68 Å, respectively, increase gradually up to pattern no. 32 (64 °C), where the intensity of the C_2AH_{10} reflections has its maximum. The Bragg reflections of C_4AH_{13} are present up to pattern no. 68 (120 °C) but have their maximum at pattern no. 52 (95 °C) at d=7.83 Å. At this temperature, the powder pattern possibly contains contributions from three crystalline solid phases, C_3AH_6, $Al(OH)_3$, and C_4AH_{13}. Table 1 lists d-spacings and relative intensities of the latter phase. The JCPDS data card # 33-255 for C_4AH_{13} has a number of lines with d-spacing values in acceptable agreement with values listed in Table 1. The final reaction product, C_3AH_6, is observed from pattern no. 27 (56 °C) and grows with depletion of C_4AH_{13}. The increase in the C_3AH_6 Bragg reflections is seen from pattern no. 52 where the quantity of C_4AH_{13} is at its maximum. The chemical reactions are reaction scheme (13) and

$$2Ca_2Al_2O_5 \cdot 8H_2O \rightarrow Ca_4Al_2O_7 \cdot 13H_2O + 2Al(OH)_3 \quad (14)$$

4. Conclusion

In the hydrothermal treatment of CAH_{10}, Figs. 1 and 2, the compound persists up to 88 °C. Then decomposition starts with formation of an amorphous phase, presumably aluminum hydroxide, and a phase with d-spacings at 3.41 and 3.28 Å, which has not been identified. Then the metastable phases C_2AH_{10} and C_4AH_{13} are formed, and ultimately the stable hydroxide C_3AH_6. This is the same sequence of events observed in the in situ hydration of cubic C_3A, extracted from cement clinker, where the first compound formed was C_4AH_{19}, followed by the compounds C_2AH_{10}, C_4AH_{13} and C_3AH_6 [8]. The hydrothermal treatment of sample B, containing C_2AH_x/C_4AH_x, Figs. 3 and 4, and sample C, containing C_2AH_8, Fig. 6, gave roughly identical reaction sequences; but the observed powder X-ray diffraction intensities from C_2AH_8 differ somewhat from the reported values. The main result is that C_3AH_6 is formed from the intermediate phase C_4AH_{13}. Fig. 3 shows formation of amorphous aluminum hydroxide, and possibly a minor quantity of gibbsite, and Fig. 6 shows only gibbsite and no amorphous aluminum hydroxide. The two experiments do not show a distinct difference between the hydrothermal reaction routes of C_4AH_{19} and C_2AH_8 to C_3AH_6. The hydrothermal hydration of C_2A, Fig. 5, results also in formation of C_2AH_8. The main final reaction products in this experiment are C_3AH_6 and gibbsite.

Acknowledgements

The Danish Natural Science Research Council has supported this investigation with grants under the program DANSYNC, and with a Steno stipend to T. R. J. The synchrotron X-ray measurements were carried out at Brookhaven National Laboratory, supported under Contract DE-AC02-98CH10886 with the US Department of Energy by its Division of Chemical Sciences Office of Basic and Energy Sciences.

References

[1] E.M. Gartner, J.F. Young, D.A. Damidot, I. Jawed, Hydration of Portland cement, in: J. Bensted, P. Barnes (Eds.), Structure and Performance of Cements, Spon Press, London, 2002, pp. 57–113.
[2] J. Bensted, Calcium aluminate cements, in: J. Bensted, P. Barnes (Eds.), Structure and Performance of Cements, Spon Press, London, 2002, pp. 114–139.

[3] E. Bleval, Gas-phase and liquid-phase hydration of C_3A, Cem. Concr. Res. 7 (1977) 297–303.
[4] E. Aruja, Unit cell and space-group determination of tetra- and di-calcium aluminate hydrates, Acta Crystallogr. 13 (1960) 1018.
[5] H.F.W. Taylor, Cement Chemistry, Academic Press, London, 1990.
[6] D.W. Foreman Jr., Neutron and X-ray diffraction study of $Ca_3Al_2(O_4D_4)_3$ a garnetoid, J. Chem. Phys. 48 (1968) 3037–3041.
[7] A.N. Christensen, M.S. Lehmann, Rate of reaction between D_2O and $Ca_xAl_yO_z$, J. Solid State Chem. 51 (1984) 196–204.
[8] A.N. Christensen, N.V.Y. Scarlett, I.C. Madsen, T.R. Jensen, J.C. Hanson, Real time study of cement and clinker phases hydration, J. Chem. Soc., Dalton Trans. (2003) 1529–1536.
[9] P. Barnes, S.M. Clark, D. Häusermann, E. Henderson, C.H. Fentiman, M.N. Muhamad, S. Rashid, Time-resolved studies of the early hydration of cements using synchrotron energy-dispersive diffraction, Phase Transit. 39 (1992) 117–128.
[10] X. Cong, R.J. Kirkpatrick, Hydration of calcium aluminate cements: a solid-state ^{27}Al NMR study, J. Am. Ceram. Soc. 76 (1993) 409–416.
[11] A.C. Jupe, X. Turrillas, P. Barnes, S.L. Colston, C. Hall, D. Häusermann, M. Hanfland, Fast in situ X-ray-diffraction studies of chemical reactions: a synchrotron view of the hydration of tricalcium aluminate, Phys. Rev., B 53 (1996) 14697–14700.
[12] P. Barnes, X. Turrillas, A.C. Jupe, S.L. Colston, D. O'Connor, R.J. Cernik, P. Livesey, C. Hall, D. Bates, R. Dennis, Applied crystallography solutions to problems in industrial solid-state chemistry. Case examples with ceramics, cements and zeolites, J. Chem. Soc., Faraday Trans. 92 (1996) 2187–2196.
[13] P. Barnes, S. Colston, B. Craster, C. Hall, A. Jupe, S. Jacques, J. Cockcroft, S. Morgan, M. Johnson, D. O'Connor, M. Bellotto, Time- and space-resolved dynamic studies on ceramic and cementitious materials, J. Synchrotron Radiat. 7 (2000) 167–177.
[14] T. Thorvaldson, N.S. Grace, V.A. Vigtusson, The hydration of the aluminates of calcium: II. The hydration products of tricalcium aluminate, Can. J. Res. 1 (1929) 201–213.
[15] E.T. Allen, H.F. Rodgers, The action of caustic hydroxides on aluminium, Am. Chem. J. 24 (1900) 304–318.
[16] G. Assarsson, Die Reaktion zwischen Tonerdezement und Wasser, Sver. Geol. Undersøkn. 27 (1933) 22–60 (Ser. C, No. 379).
[17] G. Assarsson, Untersuchungen uber Calciumaluminate: II. Die Kristallisation der Calciumaluminatlosung bei 40 °C, Z. Anorg. Allg. Chem. 205 (1932) 335–360.
[18] M.H. Roberts, New calcium aluminate hydrates, J. Appl. Chem. 7 (1957) 546–5443.
[19] N. Richard, N. Lequeux, P. Boch, Local environment of Al and Ca in CAH_{10} and C_2AH_8 by X-ray absorption spectroscopy, Eur. J. Solid State Chem. 32 (1995) 649–662.
[20] A.N. Christensen, T.R. Jensen, J.C. Hanson, Formation of ettringite, $Ca_6Al_2(SO_4)_3(OH)_{12} \cdot 26H_2O$, AFt, and monosulfate, $Ca_4Al_2O_6(SO_4) \cdot 14H_2O$, AFm-14, in hydrothermal hydration of Portland cement and of calcium aluminum oxide-calcium sulfate dihydrate mixtures studied by in situ synchrotron X-ray powder diffraction, J. Solid State Chem. 177 (2004) 1944–1951.
[21] A.N. Christensen, T.R. Jensen, N.V.Y. Scarlett, I.C. Madsen, J.C. Hanson, Hydrolysis of pure and sodium substituted calcium aluminates and cement clinker components investigated by in-situ synchrotron X-ray powder diffraction, J. Am. Ceram. Soc. 87 (2004) 1488–1493.
[22] A.P. Hammersley, S.O. Svensson, M. Hanfland, A.N. Fitch, D. Hausermann, High Press. Res. 14 (1996) 235.